doi:10.1246/cl.2011.156
156 Published on the web January 15, 2011

A Facile Synthesis of NiO Nanosheet with High-energy (111) Surface

Kake Zhu,*[1] Weiming Hua,[2] and Xingyi Wang[3]
[1]*UNILAB, Department of Chemical Engineering, East China University of Science and Technology, Shanghai 200237, P. R. China*
[2]*Shanghai Key Laboratory of Molecular Catalysis and Innovative Materials, Department of Chemistry, Fudan University, Shanghai 200433, P. R. China*
[3]*Advanced Material Lab, Research Institute of Industrial Catalysis, East China University of Science and Technology, Shanghai 200237, P. R. China*

(Received October 29, 2010; CL-100916; E-mail: kakezhu@ecust.edu.cn)

NiO nanosheet with high-energy (111) polar surface was prepared in high yield under mild conditions using nickel acetate tetrahydrate as starting material via thermal decomposition of intermediate $Ni(OH)(OCH_3)$. The NiO(111) nanosheet is far more active than conventional NiO for ethylbenzene dehydrogenation.

The activity and selectivity of a catalyst is in principle dictated by the electronic structure of the solid surface, which can be tuned by composition or physical structure at the outermost layer.[1] Surface structure control has proven to be an effective way to promote catalytic activities. It has been shown both experimentally and theoretically that metal surfaces rich in steps and low-coordinated sites with dangling bonds are active sites in catalysis,[1–3] while on metal oxides the high-energy surfaces are more favorable for heterogeneous catalysis.[4–8] Surface orientation control can endow metal oxides of earth-abundant elements with new or elevated catalytic activity. Unfortunately, high-energy surfaces are not so stable during preparation and are more likely to diminish during crystal growth, and thereby most of the exposed surfaces of conventionally prepared oxides are dominated by less reactive sites. As a result, studies on high-energy surfaces are limited to single-crystal surfaces under ultrahigh vacuum (UHV) conditions or thin films, which is particularly true for the Tasker III type surfaces of metal oxides.[9] To bridge up the pressure gap and the material gap in these studies, it is desirable to develop scalable methods to prepare metal oxides exposing mainly such high-energy surfaces.

A Tasker III surface is a surface composed of alternating positively charged anions and negatively charged cations, and a polarity is built up perpendicular to the surface. Interest in this type of surface has stemmed from the stabilization mechanism and later to their interactions with guest molecules. Attempts have been made to meet the formidable challenge to produce powder-form metal oxides exposing Tasker III type surfaces, and a few successful examples have gained attention for their novel catalytic or adsorptive properties.[6–8,10] For instance, hexagonal ZnO(0001) platelet structure with polar surface is five times more active than the rod-like ZnO with nonpolar surface in photocatalytic decomposition of Methylene Blue.[8] MgO nanosheet with (111) as major surface has exhibited superior catalytic activity in transesterification of sunflower or rapeseed oil to produce biofuels.[6,11] In these the Claisen–Schmidt condensation and transesterification have highlighted the importance of preparation methods to tailor oxides with Tasker III type high-energy surfaces, and it is still challenging to find facile methods in tailoring such surfaces.

NiO is a typical ionic oxide that possesses a rock salt structure, and the strong Coulomb attraction between cationic Ni^{2+} and anionic O^{2-} that binds them together also gives the material a high ionic character and melting point (1955 °C). NiO is an antiferromagnetic semiconductor with a wide band gap of ca. 3.6 eV[12] and is finding applications in heterogeneous catalysis,[13] electrochromic films,[14] optical fibers,[15] and Li-ion batteries.[16,17] In the rock salt structure, both the (100) and (110) surface are composed of well-balanced nickel cations and oxygen anions and are nonpolar Tasker I type surfaces.[9] The (111) surface, however, is a Tasker type III surface.[18] The NiO(111) nanosheet has exhibited superior surface activity to methanol activation and dye adsorption.[7,19]

From literature survey, it is found that NiO nanosheet structures in various forms have recently been reported. For instance, Zhu and co-workers[20] have reported β-$Ni(OH)_2$ with nanosheet structure that was prepared in mixed solvent media at 200 °C. Thermal decomposition of β-$Ni(OH)_2$ produces NiO with sheet-like morphology, but the crystalline orientation of NiO nanosheet is not preferential. Liu and co-workers[21] have prepared NiO nanosheet by means of solvent thermal synthesis under autogenic pressure at 150 °C in the presence of anionic surfactant, with $Ni_2CO_3(OH)_2$ as an intermediate. The NiO sheet preferentially grows along the nonpolar (200) and (220) facet directions. Some of us as well as Richards[7] have developed a method to prepare NiO(111) nanosheet in supercritical methanol (>245 °C), which entails high-temperature/pressure manipulations. Herein, we report a facile synthesis of NiO(111) nanosheet with Tasker III type surface under mild conditions via the formation of an intermediate $Ni(OH)(OCH_3)$ under methanol thermal conditions. Easily available nickel acetate tetrahydrate was used as a precursor, and the productivity was improved to grams level in a 130-mL autoclave due to the relatively high-concentration solution used.

To prepare NiO(111) nanosheet, 12.44 g of nickel acetate tetrahydrate (Sinopharmacy, ≥98%) was dissolved in 60.0 mL of anhydrous methanol (Sinopharmacy, ≥99.5%) and 10.82 g of benzyl alcohol (Lingfeng Chemical, ≥99%) under stirring. The resultant mixture was further stirred for 1 h to form a clear solution. The blue solution was transferred into a 130-mL Telfon-lined autoclave, which was subsequently heated in an oven at 180 °C for 36 h. A blue powder was recovered by filtration and methanol washing and air-dried overnight. Yield of the as-prepared sample is ca. 95% on a metal basis according to the composition reported.[22] The as-prepared powder was calcined in air at 550 °C for 4 h through a ramp of 3 °C min^{-1} to afford NiO(111) sheet. For comparison, NiO was also prepared via thermal decomposition of nickel nitrate under the same heating conditions.

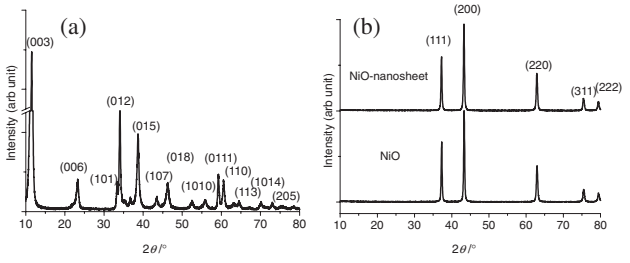

Figure 1. XRD patterns of (a) as-prepared $Ni(OH)(OCH_3)$, (b) NiO(111) nanosheet and conventional NiO.

Powder X-ray diffraction (XRD) patterns of the as-prepared and calcined samples are displayed in Figures 1a and 1b, respectively. XRD pattern of conventional NiO from nitrate thermal decomposition is also shown together with NiO nanosheet in Figure 1b. The as-prepared powder is identified as $Ni(OH)(OCH_3)$, the indexation of which is according to Le Bihan and co-workers[22] in Figure 1a. Sharpness of peaks indicates high crystallinity of $Ni(OH)(OCH_3)$. The selection rule to the structure is $-h+k=3n$ according to their hexagonal indexation, $a=0.312$ nm, $c=2.302$ nm. The structure can also be indexed to a brucite-like structure according to Kubo and co-workers,[23] who reported the synthesis of $Mg(OH)(OCH_3)$ from $Mg(OH)_2$ and believed that OCH_3^- substitutes some OH^- groups in the brucite structure and expands the lattice of crystalline $Mg(OH)_2$. Accordingly, they indexed the structure to a brucite structure. At a matter of fact, there is still no consensus on the definite structure of this metastable material, due to the small particle size that challenges X-ray determination. The structure of $Mg(OH)(OCH_3)$ is identical to that of $Ni(OH)(OCH_3)$ in crystallinity and atomic radii,[22] both are prepared via reaction between turbostratic hydrated Mg/Ni hydroxide and methanol under high temperature and pressures (for Mg, 245–315 °C and 240 bar; for Ni, 240 °C to get highly crystalline samples). From Figure 1b, it is also seen that thermal decomposition of $Ni(OH)(OCH_3)$ produces NiO with rock salt structure (JCPDS-ICDD card No. 78-0643, space group: $Fm\bar{3}m$ [No. 225]), no difference can be discerned by powder XRD between NiO nanosheet and conventional NiO from nitrate decomposition.

From TEM images of Figures 2a and 2b, it is seen that $Ni(OH)(OCH_3)$ exists in sheet-like morphologies. The sizes of these sheet range from 100 to 300 nm, and the sample unanimously has a sheet-like structure on the copper grid. In some areas overlapping of sheet can occur. As most sheet-like particles sit on the copper grid in almost all areas observed, it is difficult to identify the thickness of such sheet in TEM measurement. In field emission scanning electron microscopy (SEM) images, sheet-like morphology is more clearly seen, which is consistent with the TEM observations. The thickness of these samples can be estimated to range from 20 to 40 nm, mostly around 30 nm, as evidenced in Figures 2c and 2d. It is also seen that particle size of sheet observed in SEM is bigger than that measured by TEM, as a result of overlapping.

NiO nanosheet produced from thermal decomposition of morphology-tailored $Ni(OH)(OCH_3)$ reserves the sheet-like morphology of the as-prepared sample, as can be intuitively identified in the TEM images in Figure 3. The overall particle size of NiO is smaller than that of the intermediate $Ni(OH)(OCH_3)$, ranging from 50 nm to ca. 200 nm, as a result of the lattice shrinkage or break of crystals during thermal decomposition. Furthermore, the NiO sheet becomes more porous when the organics are removed by combustion, which is similar to what was observed for supercritically prepared material.[6,7] But the holes on these sheets are irregular in their shapes. When we zoom in each dispersed NiO sheet and do a electronic diffraction (ED) of the crystal, a characteristic diffraction pattern perpendicular to the (111) surface can be observed, as shown in the inset of Figure 3b. Overlapping of NiO sheet-like structures is more frequently observed than in $Ni(OH)(OCH_3)$, probably due to the instability of the (111) polar surfaces. The holey NiO nanosheet can also be identified from SEM images, as demonstrated in Figure 3c. From the SEM image of Figure 3d, one can see that conventional NiO has no preference in sizes and shapes, they are normally aggregated particles having various exposing facets and are much bigger in size than NiO nanosheet.

As far as the formation mechanism is concerned, the morphology control of metastable intermediate $Ni(OH)(OCH_3)$

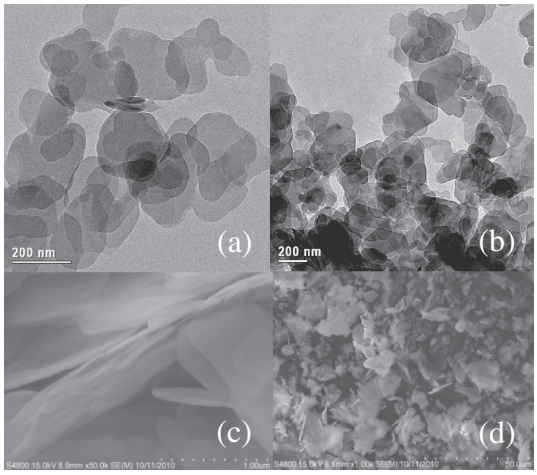

Figure 2. TEM (a, b) and SEM (c, d) images of $Ni(OH)(OCH_3)$ with sheet-like morphology.

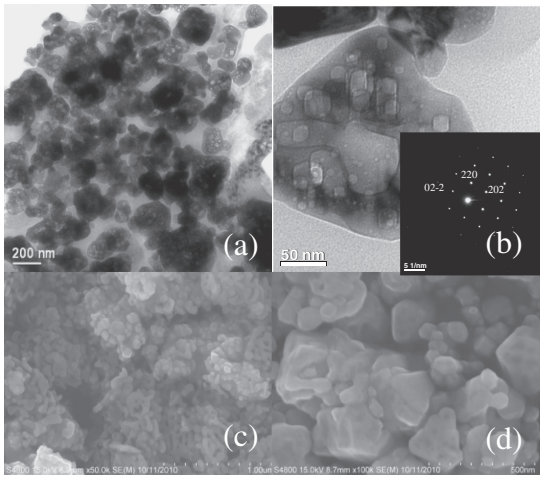

Figure 3. TEM images of NiO nanosheet (a, b) and its ED pattern (inset of b), SEM images of (c) NiO nanosheet and (d) conventional NiO.

is crucial to the rock-salt-structured NiO(111) sheet. It seems that in the presence of water and methanol in certain ratios, under either solvent thermal or supercritical conditions, $Ni(OH)(OCH_3)$ is more stable than the corresponding salt, hydroxide or methoxide. When either a solid precursor $Ni(OH)_2$ or a molecular crystal water-containing solution of nickel nitrate or acetate is adopted as precursor, $Ni(OH)(OCH_3)$ is inevitably produced. The $Ni(OH)_2$ route is a top-down method while the solution approach is bottom-up.[7,22] In the top-down method, only under rather harsh conditions $Ni(OH)(OCH_3)$ can be produced. At 200 °C, only quasi-crystalline samples can be produced, while highly crystalline $Ni(OH)(OCH_3)$ was synthesized at 240 °C. Our recent experiment has proven that it is possible to lower the temperature in the bottom-up approach to tailor the morphology of $Ni(OH)(OCH_3)$ to nanosheet. In a top-down route, the insertion of OCH_3^- ligand into the $Ni(OH)_2$ slabs to expand the lattice requires high reaction temperatures, while in a bottom-up approach the molecular build-up of $Ni(OH)(OCH_3)$ does not need such harsh conditions. The metastable $M(OH)(OCH_3)$, M = Mg, Ni, Co, etc., has not received much attention in the past for their instability; however, it can be used as an important intermediate to prepare metal oxides that expose Tasker III surfaces with sheet-like morphology.

To compare the catalytic performance of NiO(111) nanosheet with conventionally prepared NiO, the dehydrogenation of ethylbenzene was used as a model reaction. Dehydrogenation of ethylbenzene was carried out in a flow-type fixed-bed microreactor at 550 °C under atmospheric pressure. To supply the reactant, N_2 (30 mL min^{-1}) was passed through a glass evaporator filled with liquid ethylbenzene maintained at 15 °C. The catalyst load was 200 mg. The products were analyzed using an online gas chromatograph equipped with a flame ionization detector and a 2 m long stainless steel column packed with 15% DNP. Brunauer–Emmett–Teller (BET) surface areas were deduced by physisorption of nitrogen (Table 1), which gave 6.12 $m^2 g^{-1}$ for NiO(111) nanosheet and 5.19 $m^2 g^{-1}$ for conventionally prepared NiO. The surface area of NiO(111) nanosheet is not so pronounced compared with conventional NiO, which may be due to the loss of surface area during calcination at 550 °C. To exclude the effect of surface area on the acitivity, the catalytic activity is expressed as reaction rate per area unit of sample. The specific reaction rate for NiO(111) nanosheet and conventional NiO are 51 and 24 μmol $h^{-1} m^{-2}$ (Table 1), respectively, the former is 2.1 times that of the latter, indicating that the per surface area activity of the (111) surface exposing nanosheet is far more active than that of conventional NiO. To the best of our knowledge, no report on the effect of crystalline orientations on catalytic activity is available for this reaction. The surface-dependent reactivity implies that the dehydrogenation of ethylbenzene on NiO is structure-sensitive. Controlled synthesis of NiO(111) nanosheet enables us to correlate the surface structure of NiO to their catalytic activity quantitatively. Promotion or degradation of catalytic activity not only relies on active surface area but also on the specific surface orientation preference at the outermost layer. In addition, we exemplify the importance of Tasker III type NiO(111) polar surface for catalytic dehydrogenation reaction in powder form and under atmospheric pressure.

In summary, a method to synthesize NiO nanosheet exposing high-energy Tasker III type (111) surface is developed.

Table 1. Catalytic activity and surface area of NiO and NiO(111) nanosheet in dehydrogenation of ethylbenzene

Catalyst	Surface area /$m^2 g^{-1}$	Conversion /%	Reaction rate /μmol $h^{-1} m^{-2}$
NiO	5.62	5.2	24
NiO(111) nanosheet	6.19	12.0	51

The method uses nickel acetate tetrahydrate as starting material, via the formation of a sheet-like $Ni(OH)(OCH_3)$ as an intermediate, and subsequent thermal decomposition produces NiO that preserves the sheet morphology. The synthetic conditions are relatively mild, and the method can produce NiO in large quantities on a gram scale. TEM, SEM, and ED analyses corroborate that the major surface is the polar (111) surface unanimously for all sheet particles. Catalytic activity for dehydrogenation of ethylbenzene on NiO(111) nanosheet is compared with conventional NiO, and the former is 2.1 times more active than the latter. Our results show that the reaction is structure-sensitive and that Tasker III type surface orientated (111) surface is far more reactive than other surfaces.

The authors are grateful for the State Basic Research Project of China (No. 2006CB806103) and National Science Foundation of China (Nos. 21006024, 20773027, and 20633030) for financial support.

References

1 J. K. Nørskov, T. Bligaard, J. Rossmeisl, C. H. Christensen, *Nat. Chem.* **2009**, *1*, 37.
2 N. Tian, Z.-Y. Zhou, S.-G. Sun, Y. Ding, Z. L. Wang, *Science* **2007**, *316*, 732.
3 J. K. Nørskov, T. Bligaard, B. Hvolbaek, F. Abild-Pedersen, I. Chorkendorff, C. H. Christensen, *Chem. Soc. Rev.* **2008**, *37*, 2163.
4 H. G. Yang, C. H. Sun, S. Z. Qiao, J. Zou, G. Liu, S. C. Smith, H. M. Cheng, G. Q. Lu, *Nature* **2008**, *453*, 638.
5 X. Xie, Y. Li, Z.-Q. Liu, M. Haruta, W. Shen, *Nature* **2009**, *458*, 746.
6 K. K. Zhu, J. C. Hu, C. Kübel, R. Richards, *Angew. Chem., Int. Ed.* **2006**, *45*, 7277.
7 J. Hu, K. Zhu, L. Chen, H. Yang, Z. Li, A. Suchopar, R. Richards, *Adv. Mater.* **2008**, *20*, 267.
8 A. Mclaren, T. Valdes-Solis, G. Q. Li, S. C. Tsang, *J. Am. Chem. Soc.* **2009**, *131*, 12540.
9 P. W. Tasker, *J. Phys. C: Solid State Phys.* **1979**, *12*, 4977.
10 S. W. Yang, L. Gao, *J. Am. Chem. Soc.* **2006**, *128*, 9330.
11 M. Verziu, B. Cojocaru, J. C. Hu, R. Richards, C. Ciuculescu, P. Filip, V. I. Parvulescu, *Green Chem.* **2008**, *10*, 373.
12 D. Adler, J. Feinleib, *Phys. Rev. B* **1970**, *2*, 3112.
13 S. Berchmans, H. Gomathi, G. P. Rao, *J. Electroanal. Chem.* **1995**, *394*, 267.
14 E. L. Miller, R. E. Rocheleau, *J. Electrochem. Soc.* **1997**, *144*, 3072.
15 C. B. Alcock, B. Li, J. W. Fergus, L. Wang, *Solid State Ionics* **1992**, *53–56*, 39.
16 F. Jiao, A. H. Hill, A. Harrison, A. Berko, A. V. Chadwick, P. G. Bruce, *J. Am. Chem. Soc.* **2008**, *130*, 5262.
17 Y. F. Yuan, X. H. Xia, J. B. Wu, J. L. Yang, Y. B. Chen, S. Y. Guo, *Electrochem. Commun.* **2010**, *12*, 890.
18 F. Finocchi, A. Barbier, J. Jupille, C. Noguera, *Phys. Rev. Lett.* **2004**, *92*, 136101.
19 Z. Song, L. F. Chen, J. C. Hu, R. Richards, *Nanotechnology* **2009**, *20*, 275707.
20 L.-X. Yang, Y.-J. Zhu, H. Tong, Z.-H. Liang, W.-W. Wang, *Cryst. Growth Des.* **2007**, *7*, 2716.
21 L. Liu, Y. Li, S. Yuan, M. Ge, M. Ren, C. Sun, Z. Zhou, *J. Phys. Chem. C* **2010**, *114*, 251.
22 S. L. Bihan, J. Guenot, M. Figlarz, *J. Solid State Chem.* **1976**, *17*, 15.
23 T. Kubo, K. Uchida, K. Tsubosaki, F. Hashimi, *Kogyo Kagaku Zasshi* **1970**, *73*, 75.

